# Small-Angle Rayleigh Scattering in $CCl_4$ Subjected to a Temperature Gradient

G. H. Wegdam, N. M. Keulen, and J. C. F. Michielsen
*Laboratory for Physical Chemistry, University of Amsterdam, 1018 WS Amsterdam, The Netherlands*
(Received 18 March 1985)

Small-angle Rayleigh-scattering experiments have been performed in liquid carbon tetrachloride subjected to a temperature gradient. The contributions of both the heat mode as well as the viscous mode to the enhanced scattering intensity are observed. Although the observations are qualitatively in agreement with theoretical predictions, the viscous contribution is much larger than predicted.

PACS numbers: 78.35.+c, 05.70.Ln, 47.25.Qv

In recent years a large number of papers about the hydrodynamics of fluids brought into nonequilibrium stationary states by large external gradients[1-4] have been published. Starting from different assumptions the general picture emerging from all the theories is the induction of long-range correlations by the external gradients. The space and time dependence of the induced correlations effects a change in the structure factor $S(q,\omega)$, which can be written as a power series in $\nabla T/q^2$ in the case of a temperature gradient, $\nabla T$. The term proportional to $\nabla T/q^2$ corresponds to correlations parallel to the gradient and is observed as an asymmetry in the Brillouin lines of $S(q,\omega)$. Kirkpatrick, Cohen, and Dorfman[4] corrected this term for the boundary effects, which were not taken into account in the original papers.[2,3] The term has been experimentally verified by Beyssens, Garrabos, and Zalcer.[5] The next term, proportional to $(\nabla T/q^2)^2$, corresponds to long-range fluctuations perpendicular to the gradient and is the lowest-order correction to the Rayleigh line. This term was proposed by Kirkpatrick, Cohen, and Dorfman[1] and is the subject of this paper.

The full expression for the Rayleigh line as given by them is

$$S_{SS}(q,\omega)=S_T^0(q,\omega)\left[1+\frac{C_p}{T}\frac{|\nabla T|^2}{D_T^2q^4}\hat{q}_\perp^2\frac{P-2}{(P+1)(P-1)}\right]+\frac{C_p}{T}\frac{|\nabla T|^2}{D_T^2q^4}\hat{q}_\perp^2\frac{1}{(P+1)(P-1)}S_\nu^0(q,\omega), \quad (1)$$

where $\hat{q}_\perp$ is the component of the unit vector in the direction of wave vector $q$ perpendicular to $\nabla T$, $C_p$ the heat capacity, $P$ the Prandtl number $\nu/D_T$, and

$$S_T^0(q,\omega)=\rho^2k_BT\chi_T\frac{\gamma-1}{\gamma}\frac{2D_Tq^2}{\omega^2+(D_Tq^2)^2},$$

$$S_\nu^0(q,\omega)=\rho^2k_BT\chi_T\frac{\gamma-1}{\gamma}\frac{2\nu q^2}{\omega^2+(\nu q^2)^2}.$$

$S_T^0(q,\omega)$ is the well-known Rayleigh line for an equilibrium fluid. Its width is determined by the thermal diffusivity, $D_T$. In the presence of a thermal gradient its intensity is enhanced. The difference is proportional to $\nabla T^2/q^4$ and is induced by the coupling of the heat mode to the longitudinal modes. The second contribution, $S_\nu^0(q,\omega)$, in the nonequilibrium state has a width proportional to the kinematic shear viscosity. It results from the coupling between the longitudinal and transverse modes. For high Prandtl numbers the viscous contribution should be negligible according to the theory. The experiments, however, prove different. In this paper we report small-angle light-scattering experiments to verify the existence of both contributions and their $|\nabla T|^2/q^4$ dependence. In the aforementioned treatments[1-4] of nonequilibrium stationary states one assumes a fluid at rest, where heat is transported solely by conduction. The stationary state to which the description is then applicable is removed far from any hydrodynamic instability point. However, if one takes gravity into account convection will also contribute. In this case one arrives at expressions similar to (1) for the structure factor as shown by Boon and Lekkerkerker.[6] Then, the relaxation times $D_Tq^2$ and $\nu q^2$ also contain contributions proportional to $\nabla T^2/q^4$. For any experimental verification of the theories it is of utmost importance to conduct the measurements of $S(q,\omega)$ either at low Rayleigh numbers or as a function of the Rayleigh number up to its critical value as done by Allain, Cummins, and Lallemand.[7] The restriction to low Rayleigh numbers puts severe experimental conditions on a measurement of the mode-coupling contributions to $S(q,\omega)$. For a measurable change in the structure factor of a system under a temperature gradient, scattering angles of a few degrees and gradients of tens of degrees per centimeter are necessary. We have alleviated these several conditions by using the thermal-grating technique. With this technique large gradients can be achieved at low Rayleigh numbers.

The experimental setup to measure the Rayleigh line by low-angle light scattering in the presence of a large thermal gradient is schematically drawn in Fig. 1. The fluid in the scattering cell is $CCL_4$. Dust, a severe scatterer, was removed from the cell and fluid by circulating the $CCL_4$ through a 0.025-$\mu$m Teflon filter for 5 h. A parallel beam of 6 mm diam from a cw $CO_2$ laser is divided into two beams, which converge onto

 

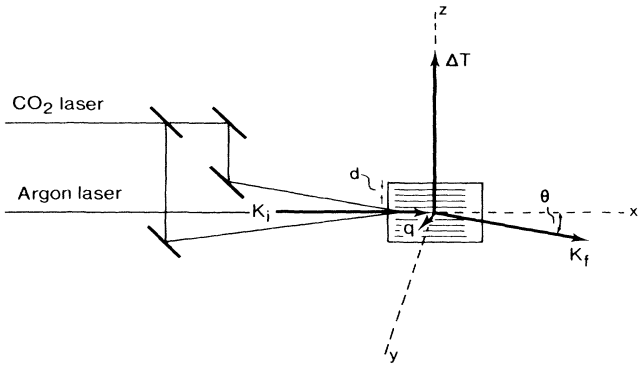


FIG. 1. Schematic drawing of the experimental setup. The wave vectors of the incident and scattered argon laser light are $k_i$ and $k_f$. The scattering angle, $\theta$, is in the $x$-$y$ plane.

the scattering cell symmetrically around the normal to the window. The interference pattern has its planes of equal phase parallel to the $x$-$y$ plane, perpendicular to the $x$-$z$ plane of the drawing. The radiation field is readily converted to a temperature field by absorption. The spatial variation is given by[8]

$$\Delta T = 2\alpha I_0 \exp(-\alpha x)\cos(kz)/\rho c_v D_T k^2, \quad (2)$$

where $I_0$ is the intensity of one $CO_2$ beam, $\alpha$ the absorption coefficient, and $k = 2\pi d$ with $d$ the grating constant. The amplitude and grating constant can be controlled by the intensity of the beams and the angle between them. A beam from a 4-W argon-ion laser propagating in the $x$-$z$ plane is focused into the scattering cell. The diameter of the waist at the focus is approximately 200 $\mu$m and determines the width of the scattering volume. Far from the cell the argon beam forms a diffraction pattern, which gives an accurate measure of the grating constant. In the measurements a grating constant of 70 $\mu$m is used. The scattering volume comprises about three periods of the temperature field in the $z$ direction. Then, the scattered light detected in the $x$-$y$ plane comes from a volume with an average temperature gradient in the $z$ direction. In addition to the sinusoidally varying gradient in the $z$ direction there is a small gradient in the $x$ direction. Inserting the appropriate numbers for $CCl_4$ into expression (2), we calculate the ratio between the gradient in the $x$ and $z$ directions to be 1%. Its relatively small value and the small angle with the scattering direction ensure that the $x$ gradient does not contribute to the enhanced scattering. However, the $x$ dependence can be used to verify the $|\nabla_z T|^2$ dependence of the enhanced scattering. By a translation of the cell with respect to the scattering center in the $x$ direction the enhanced scattering intensity, proportional to $|\nabla T|^2$ should decay as $|\nabla T|^2 \simeq \exp(-2\alpha x)$, where $x$ is the distance from the window. In the $x$-$y$ plane, going through the zeroth-order diffraction maximum, the scattering is detected. The wave vector of the scattered light is selected by slits and diaphragms and focused onto a photomultiplier. A photon correlator gives directly the density-density correlation function in the heterodyne detection mode, after subtraction of and division by the local oscillator background coming from the windows. Verification of the absence of dust and measurement of the local oscillator intensity are possible by repeating each measurement at different time scales and argon laser intensities.

In this geometry the decay time of the correlation function is measured with an accuracy of 2% for angles between 0.8 and 10 deg. A measurement of the intensity is more prone to experimental error. In the equilibrium state in the optimal optical geometry the intensity can be measured with 5% to 10% accuracy at various angles. In the nonequilibrium steady state the correlation function $C(t)$ is the sum of two exponentials. Fourier transformation of formula (1) gives

$$C_{SS}(t) = C_e(0)[1 + A(P-2)]\exp(-D_T q^2) + C_e(0) A \exp(-\nu q^2 t), \quad (3)$$

where

$$A = \frac{C_p}{T} \frac{|\nabla T|^2}{D_T^2 q^4 (P^2-1)} \hat{q}_\perp^2,$$

and $C_e(0) = \pi^2 k_B T \chi_T (\gamma - 1)/\gamma$ is the total integrated intensity of the Rayleigh line without gradients. For the total integrated intensity one obtains

$$C_{SS}(0) = C_e(0)[1 + (P-2)A] + C_e(0) A. \quad (4)$$

The second part on the right-hand side is the intensity of the fast-decaying exponential. It is independent of the temperature. The first part, however, depends upon the temperature. With the $CO_2$ laser impinging on the liquid not a temperature grating is set up; additional heating also takes place. We calculate the intensity change as a result of this to be at most 5%. A second effect of the temperature changes and gradients induced by the $CO_2$ laser is a defocusing of the argon beam. This introduces an uncertainty in intensity as well as in wave vector. According to Beyssens the influence on the wave vector is weak. The effect on the intensity is larger but difficult to assess beforehand. However, at large distances from the window and large scattering angles—small temperature gradient and large wave vectors—the equilibrium intensity is measured, provided that defocusing and heating effects are absent. From these measurements we derive that defocusing results in a 20% reduction of the intensity. All the intensities are therefore normalized by the

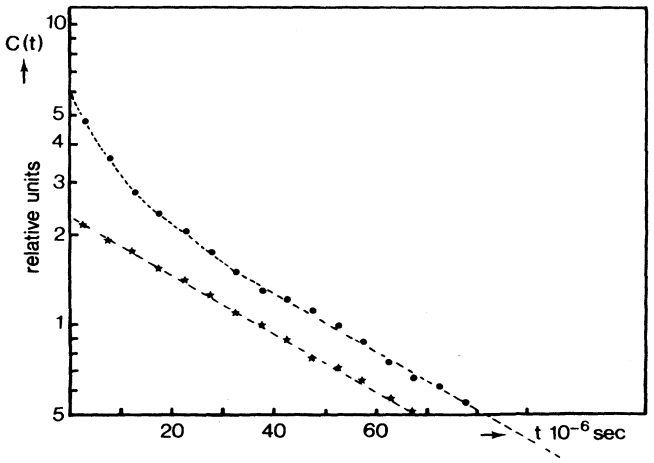


FIG. 2. Semilogarithmic plot of the measured correlation functions without (stars) and with (circles) thermal grating.

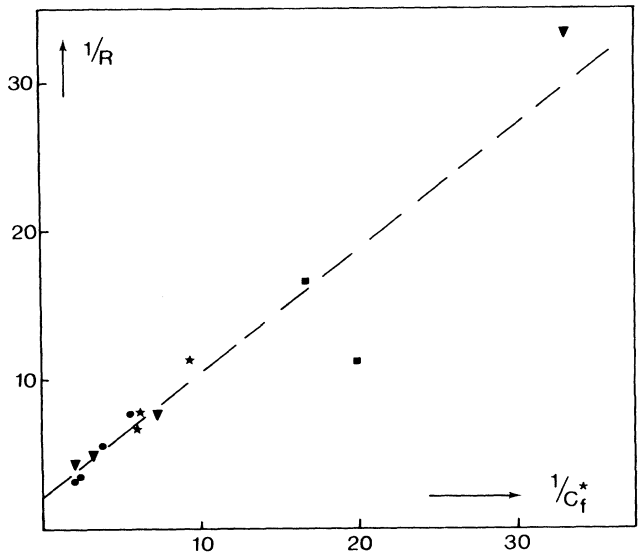


FIG. 3. Ratio of the inverse intensities of the fast to the slow component, $1/R$, as a function of the inverse intensity of the fast component. The different points correspond to different wave vectors and scattering-volume positions.

large-wave-vector, low-gradient intensities. In order to eliminate other spurious effects and optical misalignment an alternating sequence of measurements with and without grating is performed at every datum point, i.e., distance from the window and scattering angle. At regular time intervals the data are normalized on a standard intensity measurement to correct for the inevitable drift of the apparatus over the long measuring times. With these precautions the final value for the ratio of intensity enhancement to the equilibrium intensity is reliable within 20%. Since we cannot measure the thermal gradients independently, the value as such is not relevant, only the functional dependence on $\nabla T$ and $q$.

In the actual measurements $\pm 6$ W/cm$^2$ of $CO_2$ radiation was incident on a sample of $CCl_4$. With use of (2) a value for $\nabla T$ can be calculated of approximately 100 K/cm. A typical example of a measured correlation function is given in Fig. 2 on a semilog plot. With the thermal grating the correlation function is characterized by two relaxation times. The long relaxation time is equal to the equilibrium relaxation time $(D_T q^2)^{-1}$. We find a value for $D_T$ of $(7.8 \pm 0.5) \times 10^{-4}$ cm$^2$/sec for wave vectors between 900 and $7 \times 10^3$ cm$^{-1}$. The value is obtained by measuring the correlation function and the relaxation time of the zeroth-order diffraction maximum, a technique used by Allain, Cummins, and Lallemand.[7] Since the value does not depend on $q$ or $\nabla T$, convection is absent and experiments are carried out at low Rayleigh numbers.

From Fig. 2 it is clear that qualitatively all predicted features are present, e.g., an enhanced intensity with a fast and a slow component in the presence of a large gradient as given by formula (2). The fast component relaxes roughly with the expected relaxation time: $(\nu q^2)^{-1}$. Quantitatively, however, there are differences. The ratio between the slow and fast relaxation times is $5.0 = -0.5$ and independent of wave vector and measuring position in the cell. The ratio should equal the Prandtl number, which is the ratio between the kinematic viscosity and the thermal diffusivity. For $CCl_4$ the Prandtl number is 7.9.[9] The lower value in the nonequilibrium stationary state stems solely from a lower value for the kinematic shear viscosity, since the value for the thermal diffusivity remains unchanged and is equal to its classically measured value. For a discussion of the results of the measured intensities we use expression (3). The intensity ratio of the fast component to the slow component is

$$R = A/[1 + (P-2)A], \tag{5a}$$

$$1/R = 1/A + (P-2). \tag{5b}$$

In Fig. 3, $1/R$ is plotted as a function of the inverse intensity of the fast component $C_f^*(0)$, normalized by the equilibrium intensity. If defocusing is absent, all points should lie on a straight line and $A$ should be equal to $C_f^*(0)$. From the data in Fig. 3, according to relation (5b), we obtain a value for the Prandtl number of $4 \pm 0.5$. The discrepancy with the value derived from the ratio of the relaxation times can be attributed to a remainder of the defocusing effect.

The dependence on wave vector and on temperature gradient of $C_f^*(0)$ is given in Figs. 4 and 5. In Fig. 4 the change in intensity is shown as a function of the distance from the window. It should fall off as $\exp(-2\alpha d)$ according to formula (2). If the intensity is a function of $(\nabla T)$,[2] the points are obtained by normalizing all intensities for different wave vectors

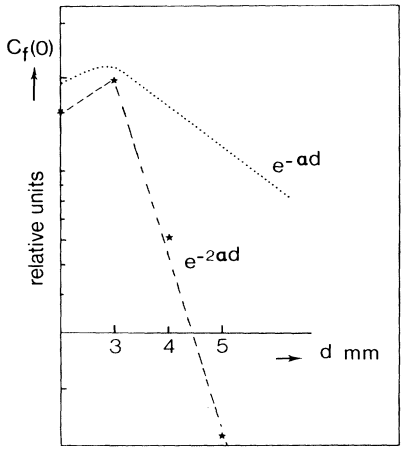


FIG. 4. Intensity of the fast component $C_f^*(0)$ as a function of the wave vector, $q$. The lines are drawn with slope $-1$. The three lines correspond to different scattering-volume positions from the window.

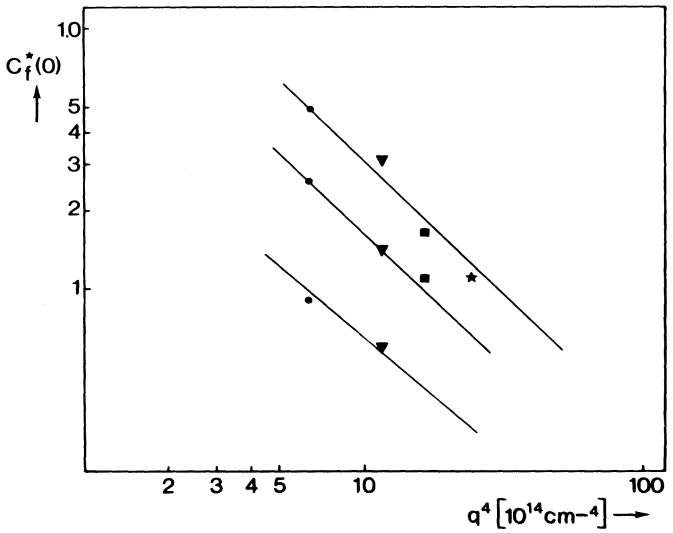


FIG. 5. Intensity of the fast component $C_f^*(0)$ as a function of the wave vector, $q$. The lines are drawn with slope $-1$. The three lines correspond to different scattering-volume positions from the window.

by the intensity of the first point and subsequently averaging over the intensities at different wave vectors. The $q^{-4}$ dependence of $C_f^*(0)$ is shown in Fig. 5 on a log-log plot. The drawn lines correspond to a few values for the temperature gradient. The values for the slopes are $-1$ indicating the $q^{-4}$ dependence. The absolute magnitude of the effect cannot be obtained reliably from the experiments. The uncertainty in the intensity measurement, but mainly the necessary normalization due to the defocusing effect, prohibits a reliable estimate. Nevertheless, the results show that by the thermal-grating technique, at low Rayleigh numbers, gradients can be induced so large that the predicted intensity enhancement can be observed at a scattering angle of a few degrees.

The main qualitative features predicted by the theory are observed: the $1/q^4$ and $\nabla T^2$ dependence of the intensity change. Surprising, however, is the observation of the fast component. Although this was predicted by the theory, we did not expect it to be observable with a Prandtl number of approximately 8. The intensity and relaxation-time ratios, however, give a Prandtl number of 4–5, because of a lower value for the kinematic shear viscosity. However, the shear viscosity for molecular systems contains two components: (a) the integral over the transverse-transverse current, and (b) the transverse–angular-momentum current correlation function. These contributions are described by Keyes and Kivelson.[10] The coupling of the orientation density to a shear gradient reduces the effective shear viscosity by 40%, practically independent of the molecular system considered.[11] The effect is observable as a dip in the depolarized Rayleigh spectrum. Here we observe in polarized scattering the longitudinal-transverse coupling which may be determined by the transverse contribution to viscosity only. A full hydrodynamic treatment may corroborate this suggestion.

This work is part of the research program of the Foundation for Fundamental Research of Matter (FOM) and the Netherlands Foundation for Chemical Research (SON), with financial aid from the Netherlands Organization for Advancement of Pure Research (ZWO).

[1]T. R. Kirkpatrick, E. G. D. Cohen, and J. R. Dorfman, Phys. Rev. A **26**, 950, 966, 972 (1980).

[2]D. Ronis, I. Procaccia, and I. Oppenheim, Phys. Rev. A **19**, 1307 1324 (1979); D. Ronis and I. Procaccia, Phys. Rev. A **26**, 1812 (1982), and **27**, 3334 (1983).

[3]G. van der Zwan, D. Bedeaux, and P. Mazur, Physica (Amsterdam) **107A**, 491 (1981).

[4]T. Kirkpatrick, E. G. D. Cohen, and J. R. Dorfman, Phys. Rev. Lett **42**, 862 (1979).

[5]D. Beyssens, Y. Garrabos, and G. Zalcer, Phys. Rev. Lett. **45**, 403 (1980).

[6]J. P. Boon and H. N. W. Lekkerkerker, Phys. Rev. A **10**, 1355 (1974), and in *Fluctuations, Instabilities and Phase Transitions,* edited by T. Riste (Plenum, New York 1975).

[7]C. Allain, H. Z. Cummins, and P. Lallemand, J. Phys. (Paris), Lett. **39**, L473 (1978).

[8]H. Eichler, G. Salje, and H. Stahl, J. Appl. Phys. **44**, 5383 (1973).

[9]*Landolt-Börnstein: Zahlenwerte und Funktionen* (Springer-Verlag, Berlin, 1972), Vol. 4, Pt. 4b, p. 563, and (1969), Vol. 2, Pt. 5a, p. 196, and (1967), Vol. 4, Pt. 4a, p. 552.

[10]T. Keyers, Phys. Rev. A **23**, 277 (1981); T. Keyes, and D. Kivelson, J. Chem. Phys. **54**, 1786 (1971).

[11]R. G. Cole, D. K. Hoffman, and G. T. Evans, J. Chem. Phys. **80**, 3565 (1984).